Progress In Electromagnetics Research, PIER 83, 173–183, 2008

HYBRID ARRAY ANTENNA FOR BROADBAND MILLIMETER-WAVE APPLICATIONS

S. Costanzo, I. Venneri, G. Di Massa, and G. Amendola

Dipartimento di Elettronica, Informatica e Sistemistica
Universitá della Calabria
87036 Rende (CS), Italy

Abstract—A hybrid array configuration suitable for wideband millimeter-wave applications is presented in this work. The proposed structure is based on the use of circular waveguide elements electromagnetically coupled trough circular apertures to a stripline distribution network. The adopted excitation mechanism avoids the use of transition components generally reducing the overall antenna efficiency. Simulated and measured results on a K_a-band prototype are discussed to prove the wideband radiation behavior.

1. INTRODUCTION

The millimeter wave portion of the electromagnetic spectrum is established today as an excellent choice to satisfy actual requirements imposed by modern wireless communication systems, such as small profile, high data rates, low cost and short radio links. As it is well known, signal wavelength becomes shorter as the frequency increases, so smaller antennas can be used at millimeter frequencies to give the required gain overcoming attenuation effects. Due to their appealing features, such as light weight, low cost, ease of fabrication and integration, planar microstrip antennas [1] are largely adopted in millimeter wave systems. However, the main disadvantage in terms of narrow bandwidth has induced researchers to look at new configurations suitable for broadband applications, such as printed dipole [2, 3] planar monopole [4–12], circular ring [13, 14] or slot [15, 16] antennas. A conformal planar array has been recently proposed [6] which combines manufacturing advantages of microstrip technology with efficiency and wideband features of waveguides. The design presented in [17] employs an array of circular waveguide radiators with a stripline distribution network fed by a rectangular waveguide. A wideband low-profile concept is demonstrated in [17], but the overall efficiency of the array is strongly limited by undesired reflections due to the presence of circular waveguides-to-stripline and stripline-to-rectangular waveguide transitions. A hybrid configuration is proposed in this work which uses an array of circular waveguides electromagnetically coupled through circular apertures to a stripline feeding network. Transition components are completely avoided, as the excitation mechanism is assured through the apertures etched on the top and the bottom ground planes of the stripline. As a consequence of this, a wide percentage bandwidth is obtained, while strongly preventing loss mechanisms. To show the effectiveness of the proposed hybrid configuration, a K_a-band prototype is completely designed, realized and experimentally tested. The large operating bandwidth is demonstrated on both the measured return loss and the radiation patterns at different operating frequencies.

2. HYBRID ARRAY CONFIGURATION AND DESIGN

The basic configuration for the single radiating element is illustrated in Figure 1, where the stripline feed is sandwiched between the top circular waveguide radiator of height h_1 and a bottom shorted circular waveguide having the same radius r and height $h_2 = \lambda_g/4$ for optimal coupling, where λ_g is the wavelength into the waveguide. The excitation mechanism is realized by electromagnetically coupling the stripline pad of dimensions W_p and L_p to the upper radiating waveguide through circular apertures of radius r etched on the top and the bottom ground planes of the stripline (Figure 1). This approach avoids the use of transition components, as those adopted in [17], so preventing undesired reflections and interactions affecting the radiator efficiency. A proper design for the single radiating element is performed by fixing the longitudinal length h_1 and the aperture radius r to simultaneously guarantee the propagation of the fundamental mode TE_{11} and the attenuation of 40 dB at least for the higher order modes. Cutoff and attenuation expressions are used at this purpose as given by the theory of standard circular waveguides [18]. Simulations on commercial computer software package Ansoft HFSS are performed to optimize the pad dimensions W_p and L_p for good matching.

On the basis of the single hybrid radiator design, a planar array of 3×6 elements (Figure 2) is considered to obtain a focused pattern in the H-plane (y-z), with a distance d along both x and y axes and a stripline power distribution network optimized by simulations to give accurate matching conditions within the operating frequency band.

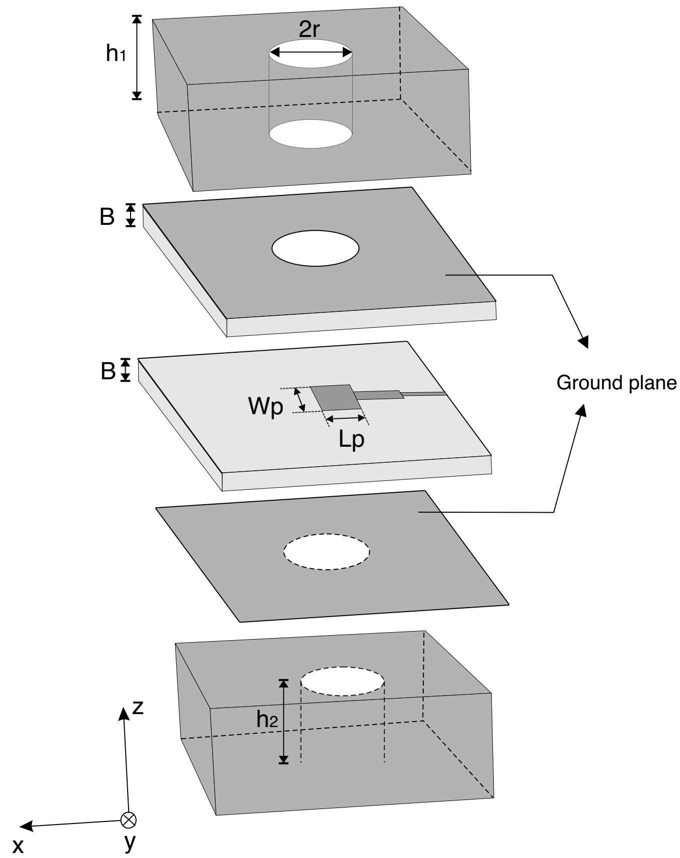

Figure 1. Geometry of the single hybrid radiator.

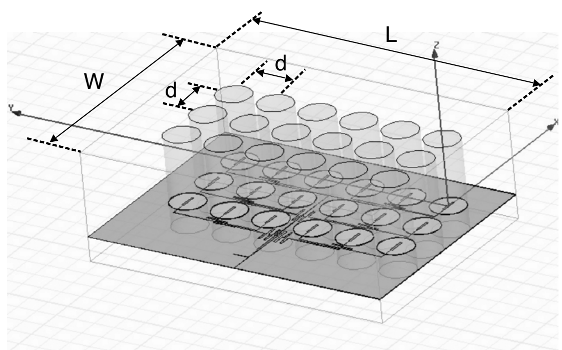

Figure 2. Hybrid array configuration.

3. NUMERICAL AND EXPERIMENTAL RESULTS

The proposed hybrid array configuration is numerically and experimentally tested on a K_a-band prototype with a central operating frequency $f_o = 30\,\text{GHz}$. First, the single radiating element is dimensioned with a longitudinal waveguide length $h_1 = 14\,\text{mm}$ and a radius $r = 3.3\,\text{mm}$ to guarantee the fundamental TE_{11} mode propagation (Figure 3) and impose a strong attenuation of higher order modes. A dielectric Arlon Diclad 870 with $\epsilon_r = 2.33$, $\tan\delta = 0.0013$ and height $2B = 0.508\,\text{mm}$ (Figure 1) is assumed for the stripline. Simulations are performed on Ansoft HFSS to optimize the pad dimensions $W_p = L_p = 0.3\,\text{mm}$ (Figure 1) for achieving good matching conditions when assuming feeding lines with characteristic impedance equal to 100Ω. The simulated return loss in Figure 4 shows a 10-dB operating bandwidth for the single radiator approximately going from 28 GHz to 31 GHz. A correct 100Ω matched impedance value can be also observed in Figure 5 at the central design frequency $f_o = 30\,\text{GHz}$. The computed co-polarized radiation patterns in the E-plane (x-z) and the H-plane (y-z) are also reported under Figure 6.

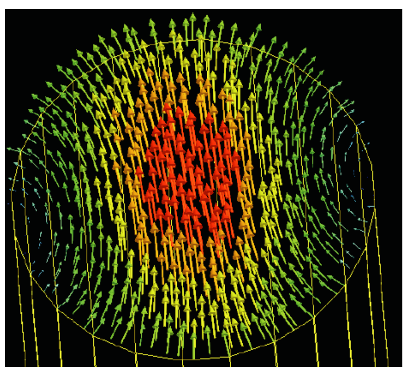

Figure 3. TE_{11} mode distribution on the circular radiating aperture (HFSS simulation).

The simulated hybrid radiator is then used as single element for the array illustrated in Figure 7, with overall dimensions $L = 59.5\,\text{mm}$, $W = 34$ mm and inter-element spacing $d = 0.85\lambda_o$ at the central frequency f_o. Pictures of the exploded view of the hybrid array and the single components are reported under Figures 8 and 9, while the feeding line network is shown under Figure 10. A satisfactory agreement between the simulated and the measured return loss of the K_a-band array can be observed in Figure 11, where the 10-dB

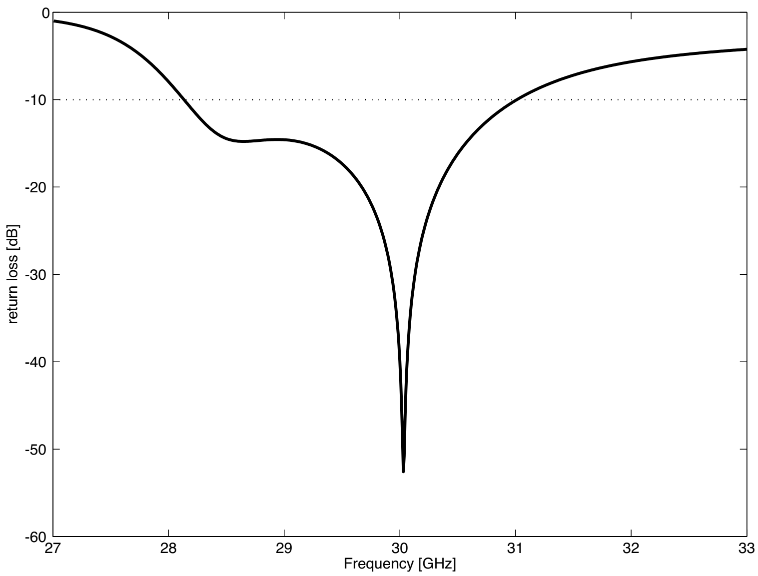

Figure 4. Simulated return loss of the single radiating element.

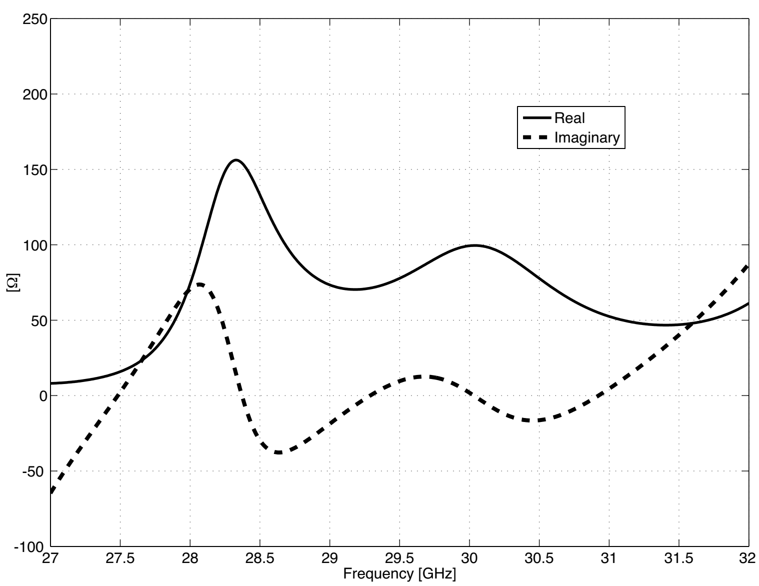

Figure 5. Simulated input impedance of the single radiating element.

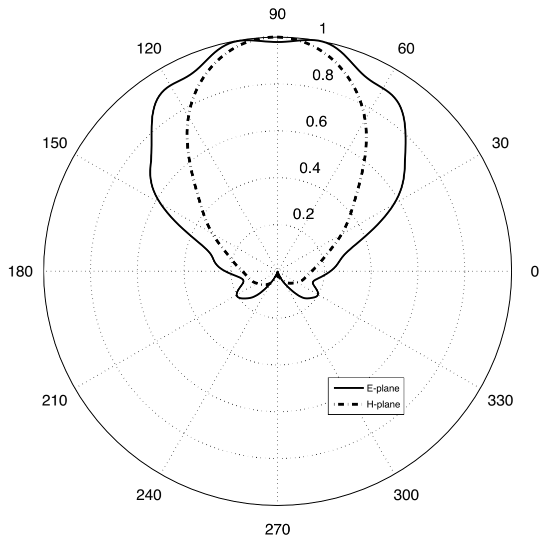

Figure 6. Computed co-polarized radiation patterns for the single radiating element.

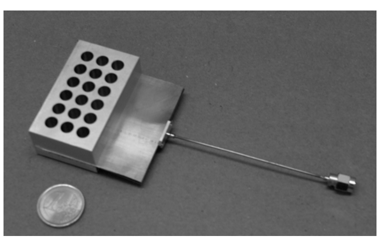

Figure 7. Picture of assembled hybrid array.

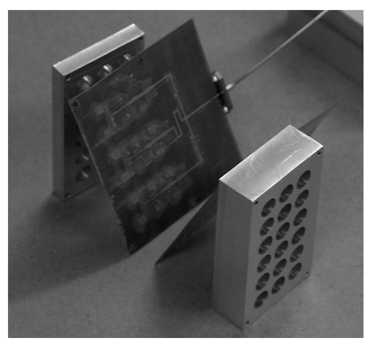

Figure 8. Exploded view of hybrid array.

bandwidth is approximately equal to 3.5 GHz (11.6%), from 28.5 GHz to 32 GHz. To further demonstrate the wideband behavior of hybrid array, far-field and gain measurements have been performed into the anechoic chamber of Microwave Laboratory at University of Calabria (Figure 12). A standard WR 28 rectangular waveguide operating in the frequency range $26.5 \div 40$ GHz has been used as measuring probe to obtain the far-field patterns of Figure 13. Similar curves with almost

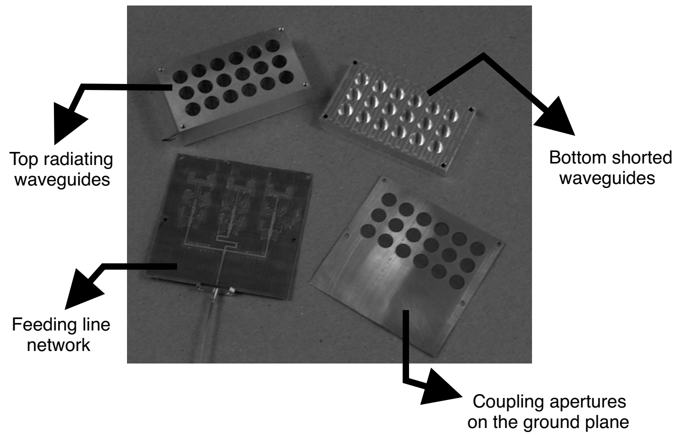

Figure 9. Single components of hybrid array.

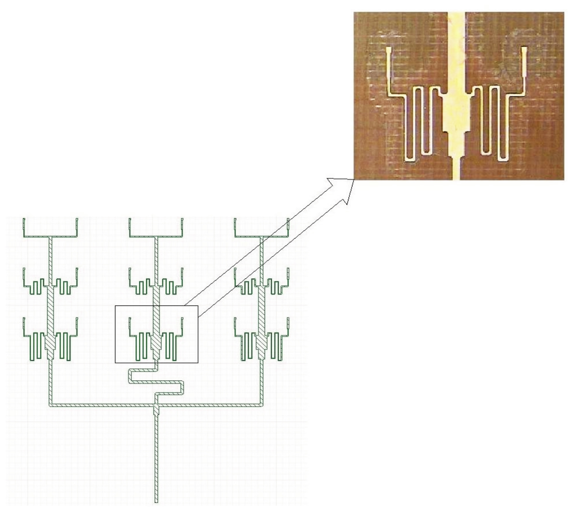

Figure 10. Feeding line network.

coincident main lobes can be observed at three different operating frequencies in the range $27.5 \div 32$ GHz. To measure the array gain, two-antenna method has been used which is based on the Friis transmission formula [19]. A calibrated pyramidal horn M.P.I. 261A/599, working in the frequency band $26.5 \div 40$ GHz, with the radiating aperture of dimensions 72.1 mm $\times$ 59.7 mm, has been used as known antenna to obtain the boresight gain of hybrid array successfully compared in

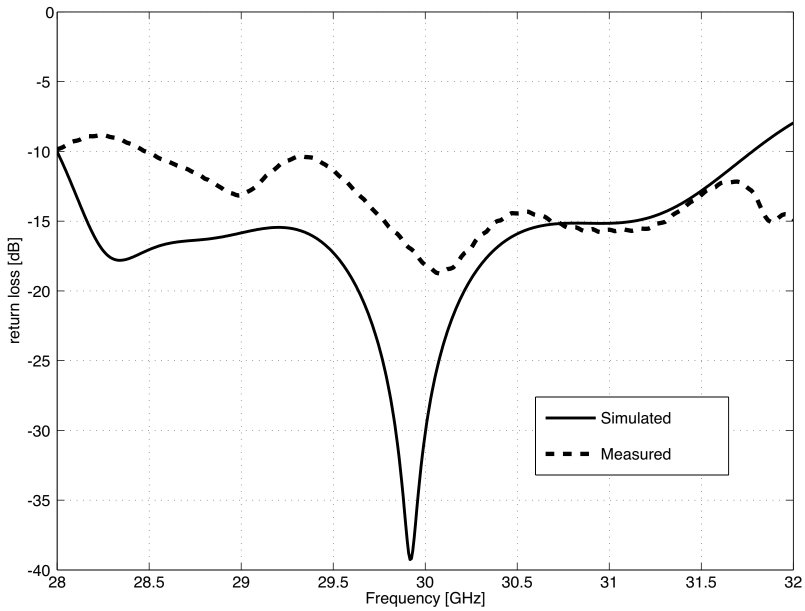

Figure 11. Measured and simulated return loss of hybrid array.

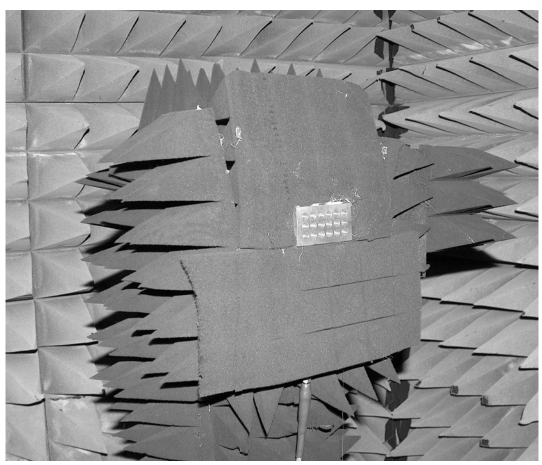

Figure 12. Picture of hybrid array into the anechoic chamber.

Figure 14 with simulation results. An average gain value of 20 dB at broadside can be observed within the operating frequency band, from 28 GHz to 32 GHz.

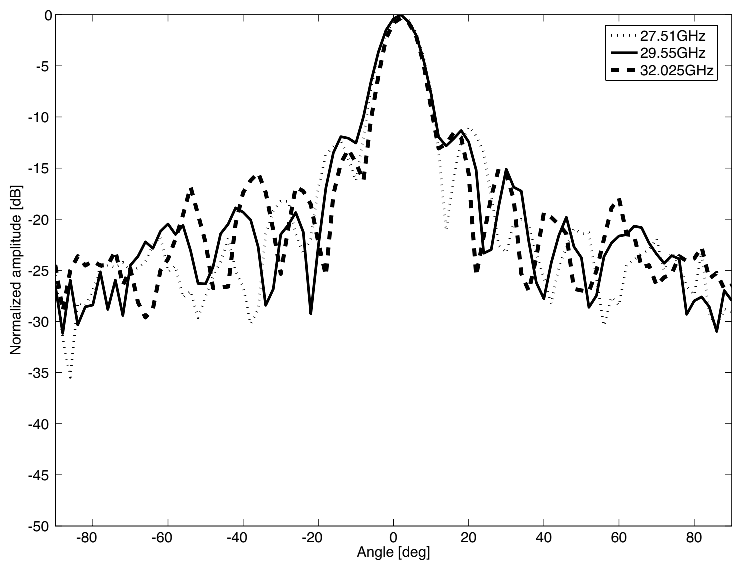

Figure 13. Measured H-plane pattern of hybrid array at different frequencies.

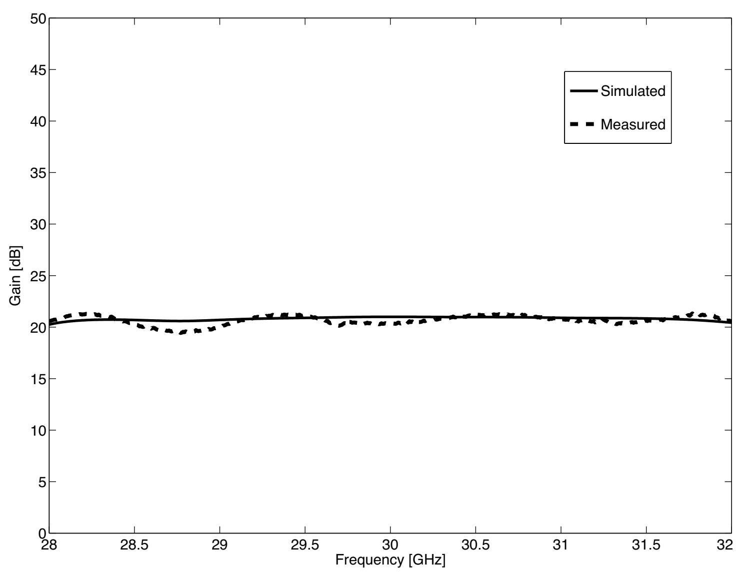

Figure 14. Measured and simulated boresight gain of hybrid array.

4. CONCLUSIONS

The use of circular waveguide radiators electromagnetically coupled to a stripline distribution network is proposed as hybrid array structure suitable for millimeter-wave applications. When compared to similar configurations existing in literature, the assumed excitation mechanism avoids the use of transition components responsible for undesired reflections. Simulated and measured results on a K_a-band prototype are discussed to show the wideband radiating behavior of the proposed array configuration.

REFERENCES

1. Pozar, D. M., *Microstrip Antennas: The Analysis and Design of Microstrip Antennas and Arrays*, IEEE Press, New York, 1995.
2. Kuo, L.-C., H.-R. Chuang, Y.-C. Kan, T.-C. Huang, and C.-H. Ko, "A study of planar printed dipole antennas for wireless communication applications," *Journal of Electromagnetic Waves and Applications*, Vol. 21, No. 5, 637–652, 2007.
3. Wang, F. J. and J.-S. Zhang, "Wideband printed dipole antenna for multiple wireless services," *Journal of Electromagnetic Waves and Applications*, Vol. 21, No. 11, 1469–1477, 2007.
4. Shan, D. M., Z. N. Chen, and X. H. Wu, "Signal optimization for UWB radio systems," *IEEE Trans. Antennas Propag.*, Vol. 53, 2178–2184, 2005.
5. Ren, W., Z.-G. Shi, and K. S. Chen, "Novel planar monopole UWB antenna with 5-GHz band-notched characteristic," *Journal of Electromagnetic Waves and Applications*, Vol. 21, No. 12, 1645–1652, 2007.
6. Fu, F., L. Yan, K. Huang, and J. Dong, "Design and implement of a CPW-fed meander monopole antenna with V-shape notched ground for WLAN," *Journal of Electromagnetic Waves and Applications*, Vol. 21, No. 14, 2129–2136, 2007.
7. Zhang, G.-M., J.-S. Hong, B.-Z. Wang, Q.-Y. Qin, B. He, and D.-M. Wan, "A novel planar monopole antenna with an H-shaped ground plane for dual-band WLAN applications," *Journal of Electromagnetic Waves and Applications*, Vol. 21, No. 15, 2229–2239, 2007.
8. Peng, L. and C.-L. Ruang, "A microstrip fed monopole patch antenna with three stubs for dual-band WLAN applications," *Journal of Electromagnetic Waves and Applications*, Vol. 21, No. 15, 2359–2369, 2007.

9. Liu, W. C. and C.-F. Hsu, "CPW-fed notched monopole antenna for UMTS/IMT-2000/WLAN applications," *Journal of Electromagnetic Waves and Applications*, Vol. 21, No. 6, 841–851, 2007.
10. Ren, W., J. Y. Deng, and K. S. Chen, "Compact PCB monopole antenna for UWB applications," *Journal of Electromagnetic Waves and Applications*, Vol. 21, No. 10, 1411–1420, 2007.
11. Liu, Y.-T., "Wideband omnidirectional operation monopole antenna," *Progress In Electromagnetics Research Letters*, Vol. 1, 255–261, 2008.
12. Yin, X.-C., C.-L. Ruan, C.-Y. Ding, and J.-H. Chu, "A planar U type monopole antenna for UWB applications," *Progress In Electromagnetics Research Letters*, Vol. 2, 1–10, 2008.
13. Ren, Y.-J. and K. Chang, "An ultrawideband microstrip dual-ring antenna for millimeter-wave applications," *IEEE Antennas and Wireless Propagat. Letters*, Vol. 6, 457–459, 2007.
14. Yang, G.-M., R. Jin, J. Geng, and W. He, "Planar broadband millimeter-wave antenna based on open loop ring resonators," *Microwave and Optical Technology Letters*, Vol. 50, No. 2, 324–328, 2008.
15. Chen, Y.-L., C.-L. Ruan, and L. Peng, "A novel ultra-wideband bow-tie slot antenna in wireless communication systems," *Progress In Electromagnetics Research Letters*, Vol. 1, 101–108, 2008.
16. Lao, J., R. Jin, J. Geng, and Q. Wu, "An ultra-wideband microstrip elliptical slot antenna excited by a circular patch," *Microwave and Optical Technology Letters*, Vol. 50, No. 4, 845–846, 2008.
17. Navarro, J., "Wide-band, low-profile millimeter-wave antenna array," *Microwave and Optical Technology Letters*, Vol. 34, No. 4, 253–255, 2002.
18. Balanis, C. A., *Advanced Engineering Electromagnetics*, John Wiley and Sons, New York, 1989.
19. Balanis, C. A., *Antenna Theory: Analysis and Design*, John Wiley and Sons, New York, 1997.